Supplementary material

Vanadium niobium carbide ($VNbCT_x$) bimetallic MXene derived V_5S_8-Nb_2O_5 @MXene heterostructure for efficiently boosting the adsorption and catalytic performance of lithium polysulfide

Yuqing Chen [a, d], Yongjie Huang [a, b], Qing Xu [a, d], Liying Yang [a, b] *, Ningyi Jiang [c] *, Shougen Yin [a,b]

[a] Key Laboratory of Display Materials and Photoelectric Devices (Ministry of Education) and Tianjin Key Laboratory for Photoelectric Materials and Devices, Tianjin University of Technology, Tianjin 300384, China

[b] School of Materials Science and Engineering, Tianjin University of Technology, Tianjin 300384, China

[c] Institute for New Energy Materials & Low-Carbon Technologies, Tianjin University of Technology, 300384 Tianjin, China

[d] Tianjin Key Laboratory of Quantum Optics and Intelligent Photonics, School of Science, Tianjin University of Technology, Tianjin 300384, China

*Corresponding authors: L.Y. Yang & N.Y. Jiang

Email: liyingyang@tjut.edu.cn; nyjiang@email.tjut.edu.cn

1. Experimental section

1.1 Lithium polysulfide (LiPS) adsorption tests

1.1.1 Preparation of Li_2S_6 stock solution

Li_2S and sublimed S were combined in a mole ratio of 1:5, respectively, in a 1:1 (V/V) solution of 1,3-dioxolane (DOL) and dimethoxyethane (DME) to prepare a Li_2S_6 stock solution with an initial concentration of 0.25 M. The mixture was stirred gently at 70 °C for 24 h to ensure complete mixing and reaction. The Li_2S_6 stock solution was subsequently diluted to the desired concentration for the adsorption tests.

1.1.2 Visual assessment of polysulfide adsorption

To visually assess the polysulfide adsorption of different candidate materials, 20 mg of $VNbCT_x$ ($VNbO_5$@MX or V_5S_8-Nb_2O_5@MX) was placed in 5 mL of a 2.5 mM Li_2S_6 solution. After the resting period of 24 h in the Li_2S_6 solution, a photograph was taken to capture any visible changes in the appearance of the Li_2S_6 solution consisting of different candidate materials.

1.1.3 Adsorption isotherm and kinetic studies

The amount of candidate material utilized was 20 mg, which remained the same for both tests. In the kinetic study, the adsorption of polythiols was investigated over time, with candidate material being exposed to a lithium polythiol solution for varying durations (2 h, 6 h, 12 h, and 24 h), while maintaining the initial concentration of the lithium polythiol solution constant at 5 mM. Adsorption equilibrium was reached at each time point. In studies of adsorption isotherms (the relationship between polysulfide adsorption and

concentration), the immersion time (24 h) and the initial molar number of LiPS (25 μmol) are kept constant. By adjusting the volume of the DME/DOL solvent (from 50 to 5 mL), the concentration (from 0.5 to 5 mM) is varied to maintain a consistent amount of polysulfide. After each adsorption test, the supernatant is collected to determine the remaining concentration of polysulfide in the solution, thereby assessing the adsorption capacity of the candidate material under specific conditions.

1.2 Li_2S nucleation tests

$VNbCT_x$, $VNbO_5$@MX and V_5S_8-Nb_2O_5@MX were dispersed in ethanol and then coated on a carbon-containing aluminium foil as a cathode with the same loading of 1 mg cm^{-2}. Li foil and Celgard 2500 film were used as the anode and diaphragm, respectively. Then, 20 μL of 0.2 M Li_2S_8 electrolyte prepared by dissolving Li_2S and sulfur in tetraethyleneglycol dimethyl ether at a molar ratio of 1:7 and heating under stirring at 65 °C for 24 h was added dropwise to the cathode. At same time, 20 μL of blank electrolyte was added dropwise to the Li anode side. For Li_2S nucleation tests, all cells were discharged to 2.06 V at a constant current of 0.112 mA, and then kept discharged at a constant potential at 2.05 V to drive Li_2S nucleation until the current dropped to less than 10^{-5} A. The Li_2S nucleation tests were carried out on the anode side of the cells.

1.3 Li–S cells assembly and electrochemical measurements

The cathodes were prepared by homogeneously mixing S/$VNbCT_x$, S/$VNbO_5$@MX or S/V_5S_8-Nb_2O_5@MX (70 wt%) with conductive carbon (20 wt%) and polyvinylidene difluoride (PVDF) as binder (10 wt%) in N-methyl-2-pyrrolidone (NMP). The resulting paste was then coated on a piece of Al foil

and vacuum dried at 50 °C for 24 h. 1 M bis (trifluoromethanesulfonyl) imide lithium (LiTFSI) and 1 wt% $LiNO_3$ were dissolved as additives in a mixture of DOL and DME (V/V=1:1). Li foil and Celgard 2500 film were used as anode and diaphragm, respectively. When the mass load of sulfur is 1.5 mg cm^{-2}, the mass ratio of electrolyte to active sulfur is 10 μL mg^{-1}. Once the mass load of S increases to 3.25, 4.32, and 5.75 mg cm^{-2}, the electrolyte concentration decreases to 8, 6, and 5 μ L mg^{-1}. Cyclic voltammetry (CV) measurements were performed at a scan rate of 0.1 mV s^{-1} in the potential range of 1.7 - 2.8 V (vs. Li^+/Li) on a CHI760E electrochemical workstation. Electrochemical impedance spectroscopy (EIS) was collected in the frequency range of 100 kHz to 0.01 Hz. Cycling performance was performed between 1.7 V and 2.8 V at room temperature using a battery test system (LAND CT3001A). The cells were activated for three cycles at 0.1 C before long-term cycling at 0.2 and 1 C. Here, 1 C corresponds to a current density of 1,675 mAh g^{-1}.

2 Density functional theory (DFT) computational analysis

From the Materials Project website, we acquired the necessary crystal structures of MXene ($VNbCT_x$), Nb_2O_5, and V_5S_8. Utilizing the Vesta and MS software, we constructed models of the crystal structures. Our fundamental construction of the crystal structure was centered on a 4×4 supercell comprising 80 atoms. Following optimization, the side and top views of the MXene ($VNbCT_x$) model structure are depicted in Fig. S1a. For V_5S_8, we built a 1×2 supercell structure oriented in the (002) direction, and for Nb_2O_5, a 1×3 supercell structure in the (001) direction, both in alignment with the XRD PDF cards. After modeling and optimization, the side and top views of the V_5S_8 and

Nb_2O_5 model structures are illustrated in Figs. S1(b-c). Subsequently, we integrated the 1×2 supercell of V_5S_8 (002) with the 1×3 supercell of Nb_2O_5 (001) to form a heterostructure, with the optimized side and top views of the V_5S_8-Nb_2O_5 heterostructure model shown in Fig. S1d. We used the DFT as implemented in the Vienna Ab initio simulation package (VASP) in all calculations. The exchange-correlation potential is described by using the generalized gradient approximation of Perdew-Burke-Ernzerhof (GGA-PBE). The projector augmented-wave (PAW) method is employed to treat interactions between ion cores and valence electrons. The plane-wave cutoff energy was fixed to 450 eV. Given structural models were relaxed until the Hellmann-Feynman forces smaller than -0.02 eV/Å and the change in energy smaller than 10^{-5} eV was attained. Grimme's DFT-D3 methodology was used to describe the dispersion interactions among all the atoms in adsorption models. The adsorption energy is defined as:

$$Eads = E(system)-E(catalyst) -E(species)$$

Where, E(system), E(catalyst), and E(species) are the total energy of the optimized system with adsorbed species, the isolated catalyst, and species, respectively.

3 Characterization

The morphology of the as-prepared $VNbCT_x$ MXene, $VNbO_5$@MX, V_5S_8-Nb_2O_5@MX was observed using a scanning electron microscopy (SEM, Hitachi SU8010). Thermogravimetric (TG) analysis was carried using a thermal analyzer (Shimadzu TA-50) with a heating rate of 10 °C min^{-1} under Ar

atmosphere. Powder X-ray diffraction (XRD) patterns were collected using a SmartLab 9KW diffractometer with Cu (λ=1.54118 Å) radiation in the range from 3 ° to 80 ° (2θ) at 293 K. The Brunauer-Emmett-Teller (BET) surface area and the N_2 adsorption-desorption isotherms were measured on a gas adsorption analyzer (Quantachrome Autosorb-IQ3+ChemStar). X-ray photoelectron spectroscopy (XPS) analysis of the samples was performed using a Thermo Scientific ESCA LAB250Xi spectrometer with an excitation source of Al Kα. The Mecasys Optizen POP UV-Vis spectrophotometer is used to measure the absorbance spectrum within the wavelength range of 280 to 800 nm, and the absorbance values are recorded.

4 Supporting Figures

(a)：MXene($VNbCT_x$)

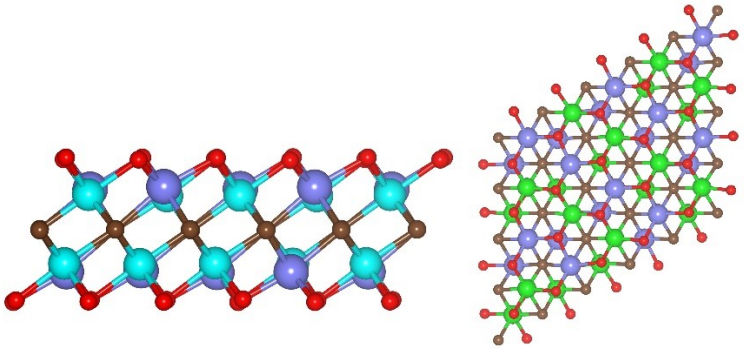

(b)：Nb_2O_5

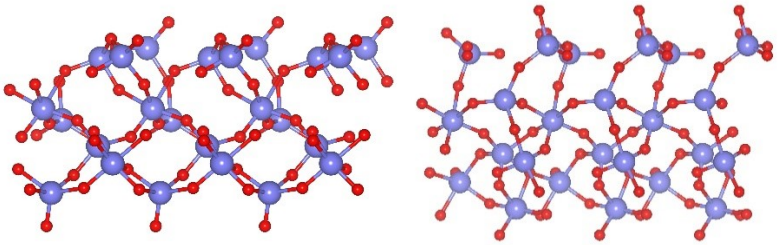

(c)：V_5S_8

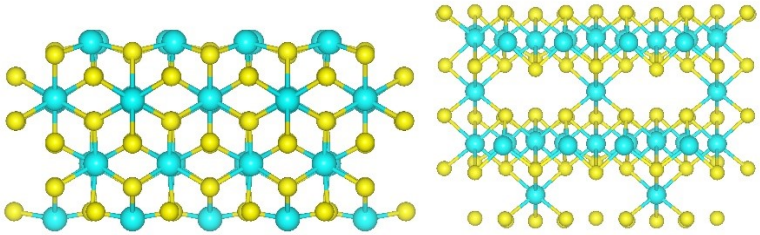

(d) : V_5S_8- Nb_2O_5

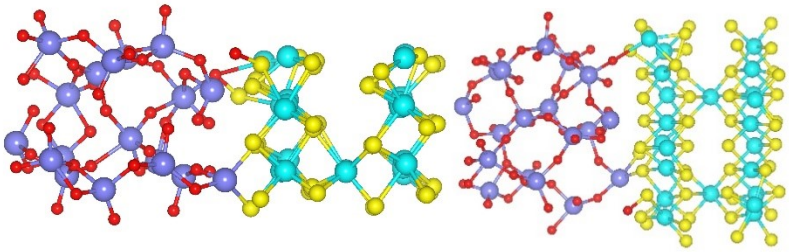

Fig. S1 The optimized structures of (a) MXene ($VNbCT_x$) (b)Nb_2O_5 (c) V_5S_8 (d) V_5S_8- Nb_2O_5 models (side and top views).

Fig. S2 SEM image of V_5S_8-Nb_2O_5 @MX

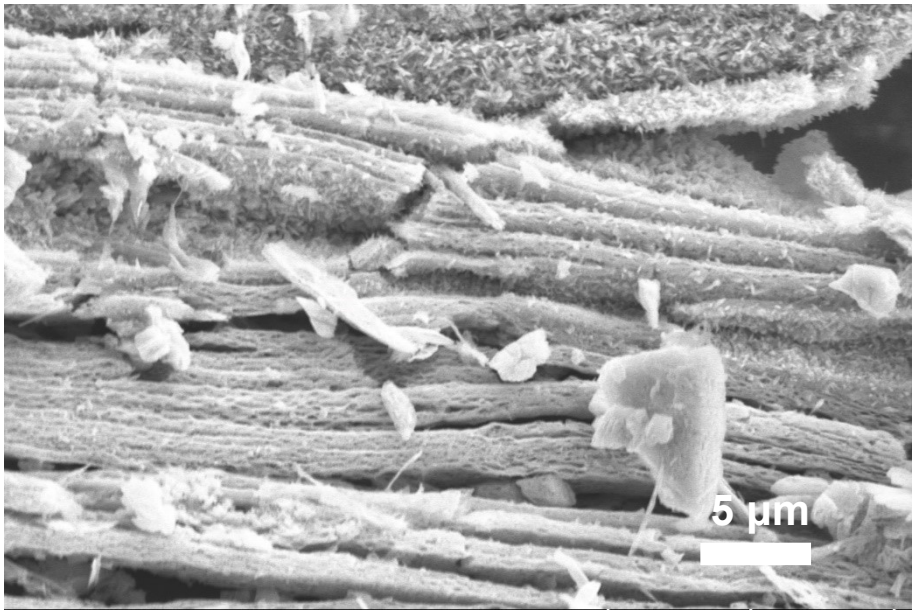

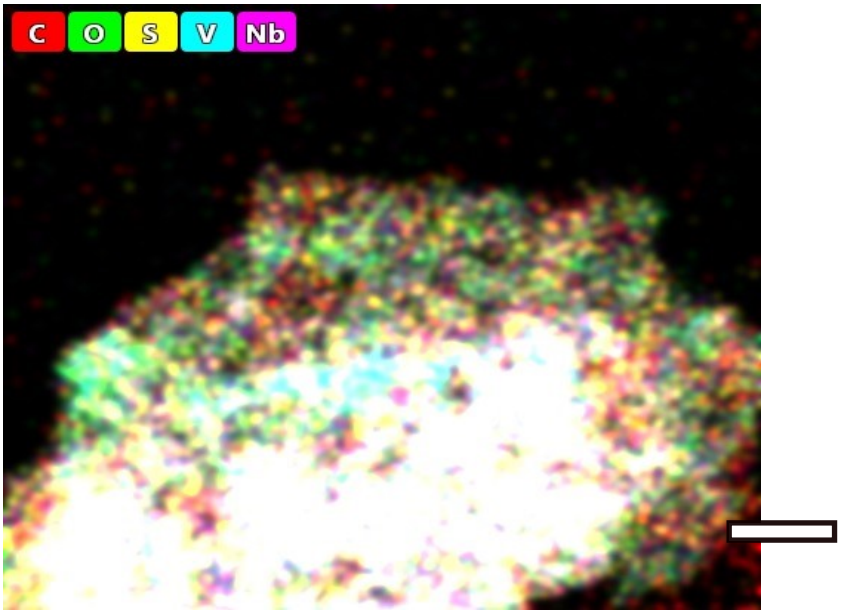

Fig. S3 Corresponding elemental mappings of overlap.

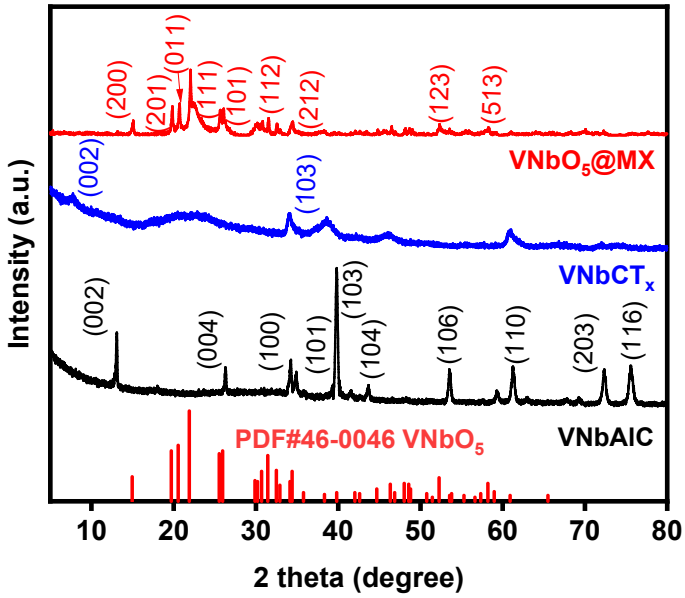

Fig. S4 XRD patterns of VNbAlC, $VNbCT_x$ and $VNbO_5$@MX.

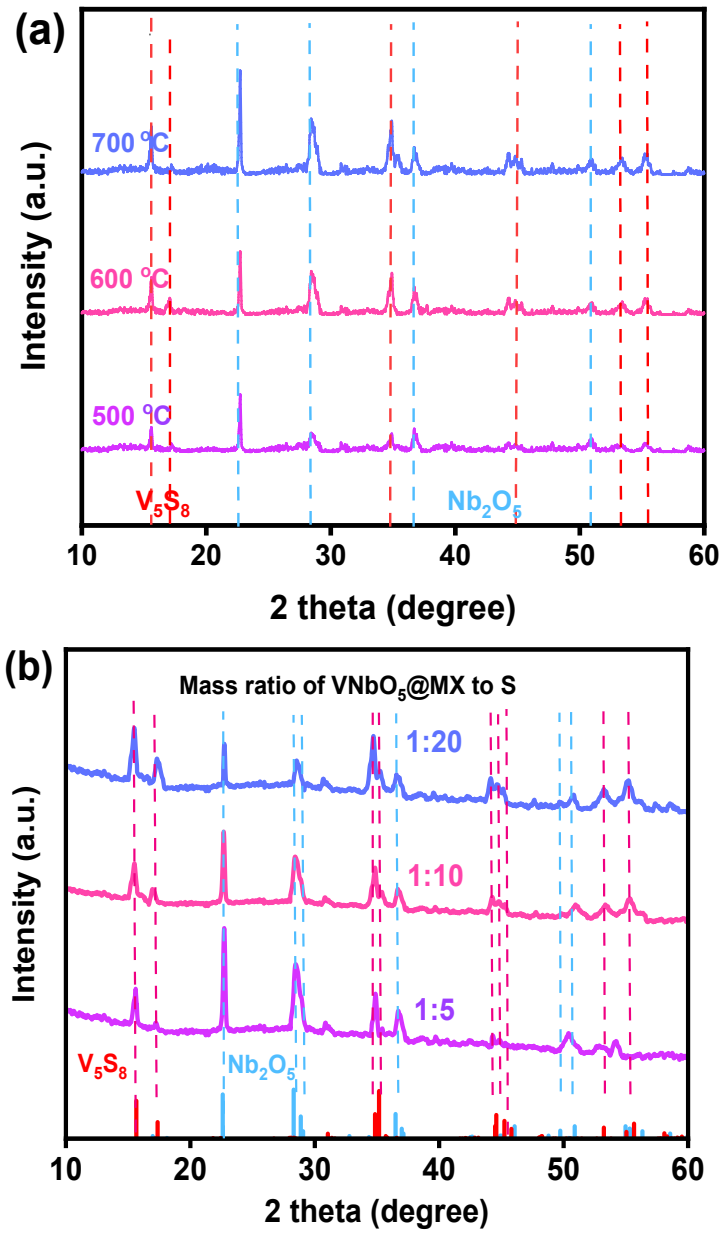

Fig. S5 XRD patterns of V_5S_8-Nb_2O_5@MX synthesized at different temperature (a) and different feeding ratios of $VNbO_5$@MX to S (b).

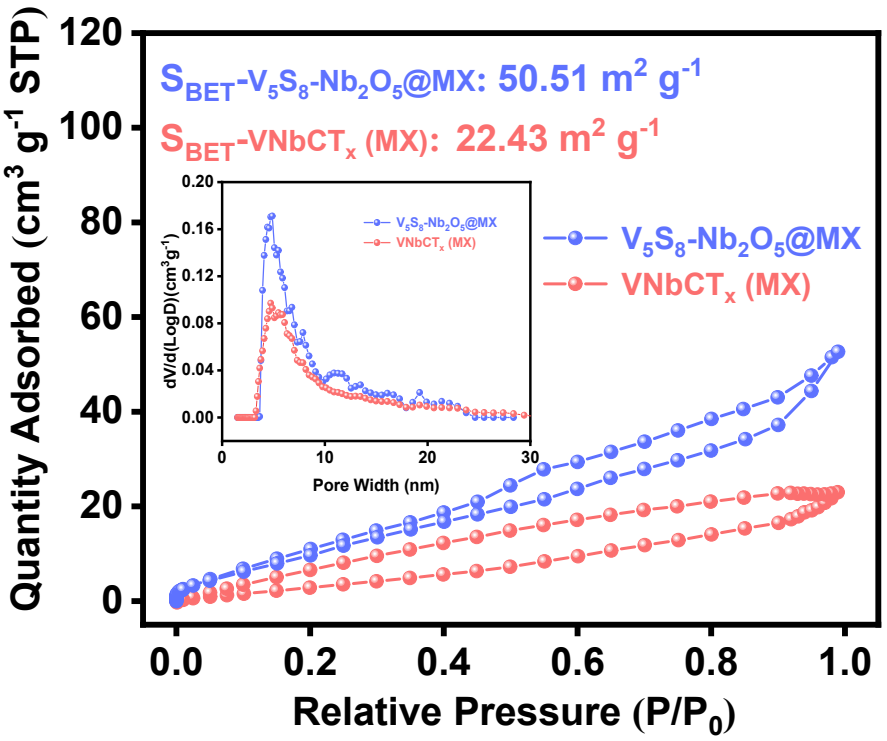

Fig. S6 N_2 adsorption and desorption isotherms and corresponding pore size distribution curve of V_5S_8-Nb_2O_5@MX and $VNbCT_x$(MX).

.

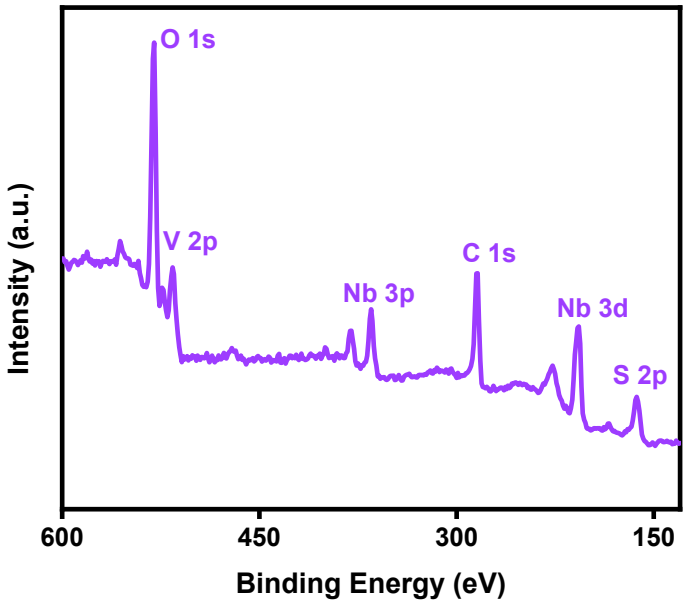

Fig. S7 XPS full scan spectrum of V_5S_8-Nb_2O_5@MX.

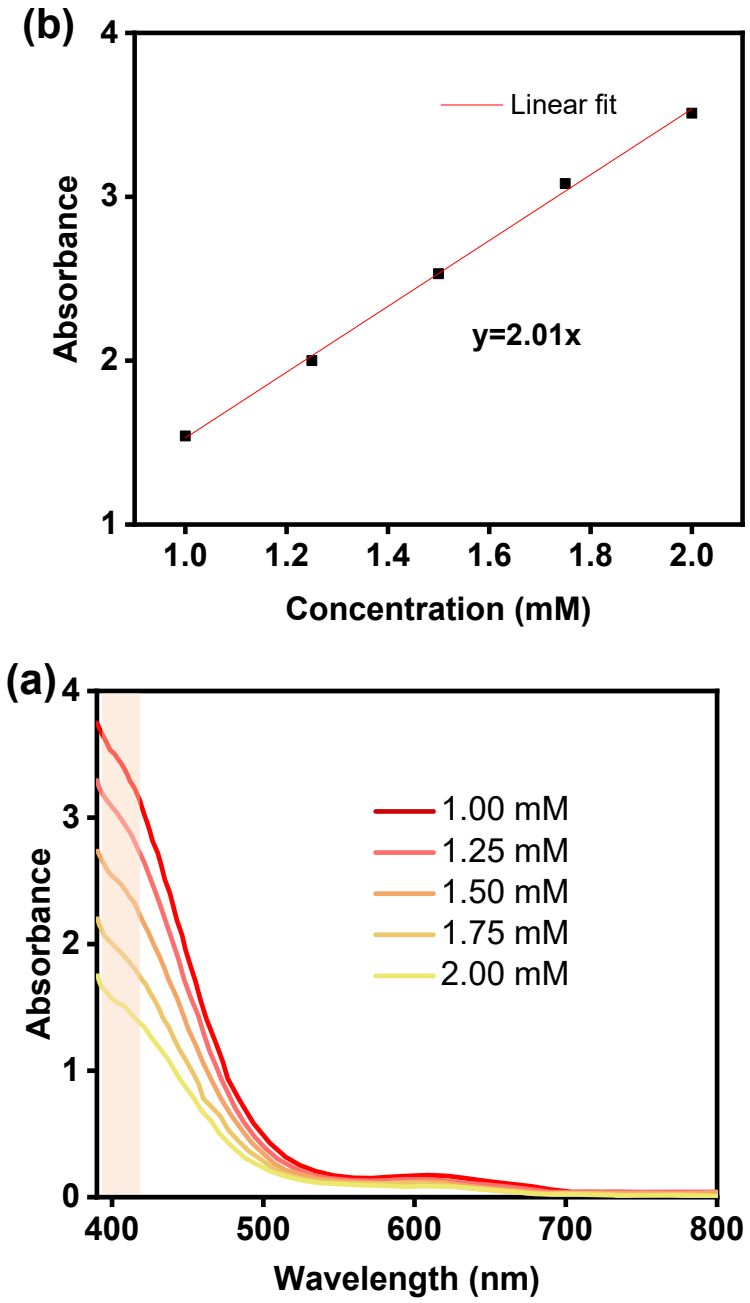

Fig. S8 (a) UV-vis absorption spectra of different concentrations of Li_2S_6 in 1:1 DME/DOL mixed solvent. Inset showing the color variation of Li_2S_6 solution with changing concentrations. (b) Calibration curve of absorbance vs. Li_2S_6 concentration (measured at a wavelength of 400 nm). The absorbance (A) and concentration (C) are related by the expression: A = ε * L * C, where the value of ε * L is 2.01, a constant derived from the calibration curve.

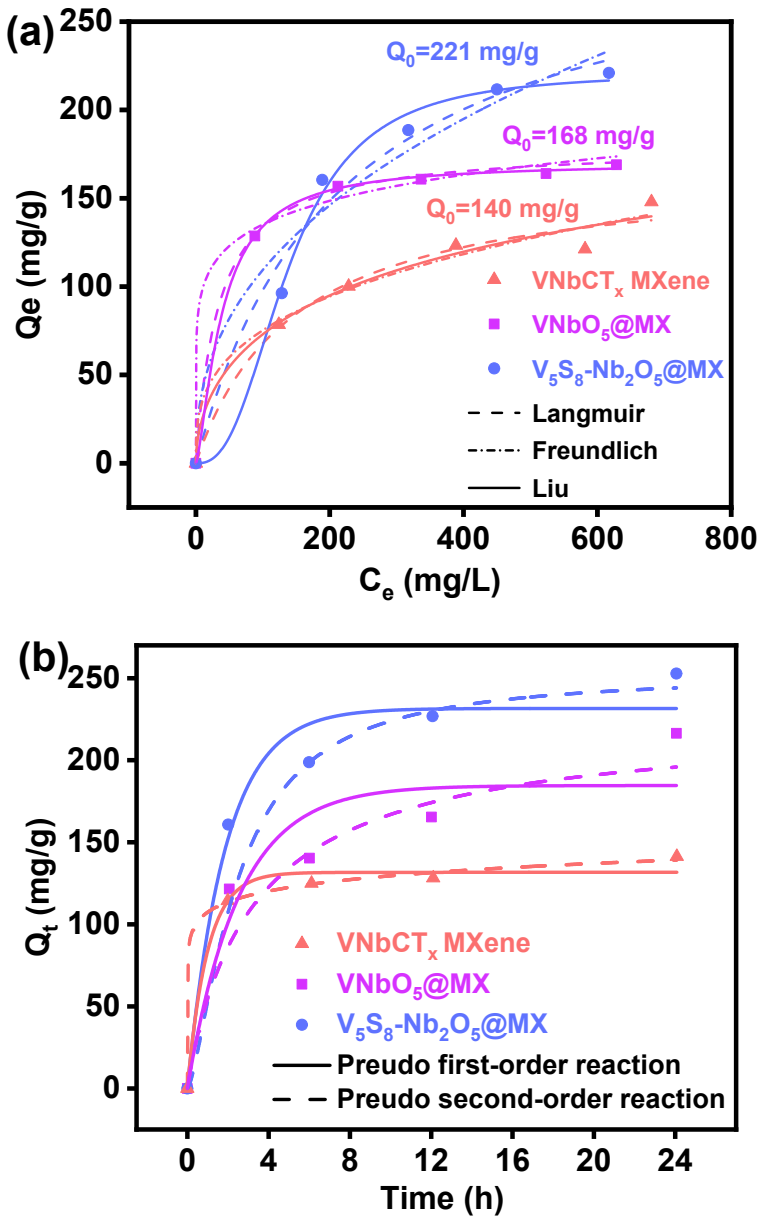

Fig. S9 (a) Adsorption isotherms and (b) adsorption kinetics curves of the $VNbCT_x$, $VNbO_5$@MX and V_5S_8-Nb_2O_5@MX.

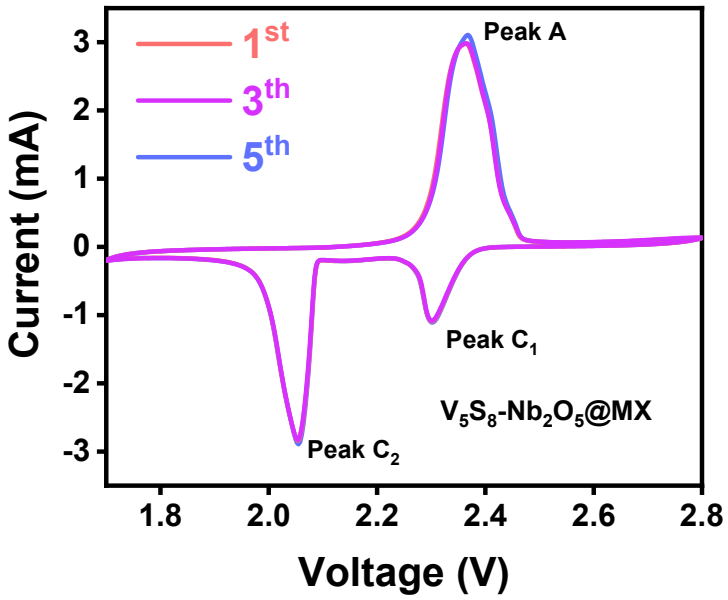

Fig. S10 Selected CV curves for different cycles.

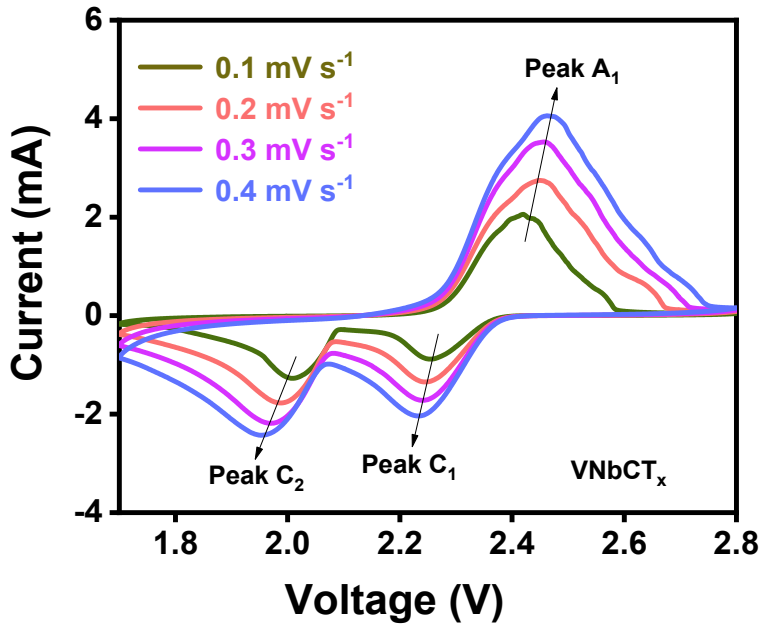

Fig. S11 $VNbCT_x$ electrode at different scan rates from 0.1-0.4 mV s^{-1}.

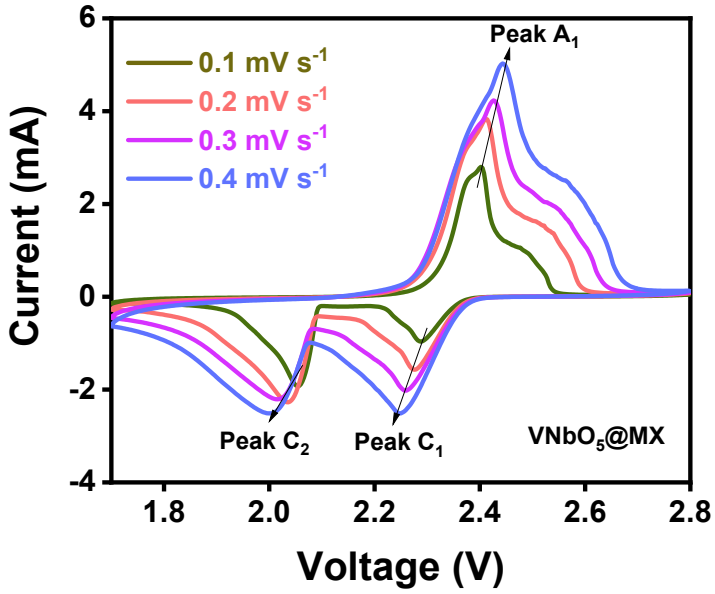

Fig. S12 $VNbO_5$@MX electrode at different scan rates from 0.1-0.4 mV s^{-1}.

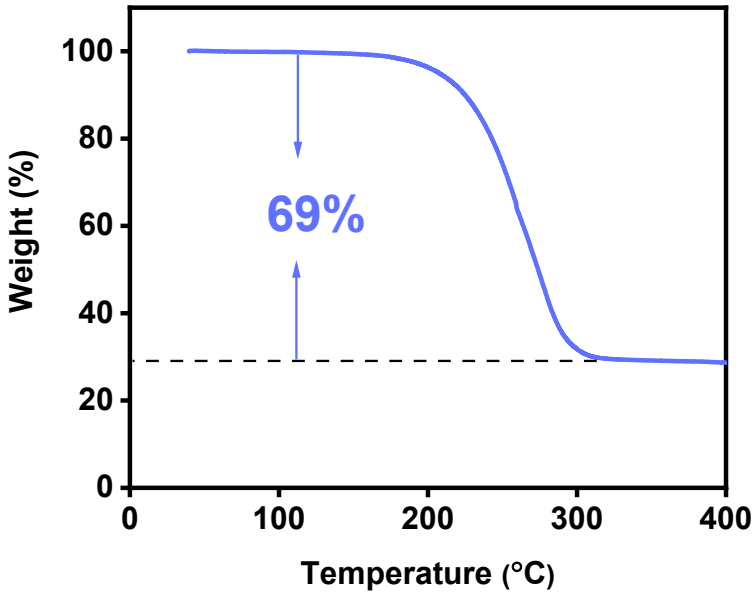

Fig. S13 TGA curves of S/V_5S_8-Nb_2O_5@MX.

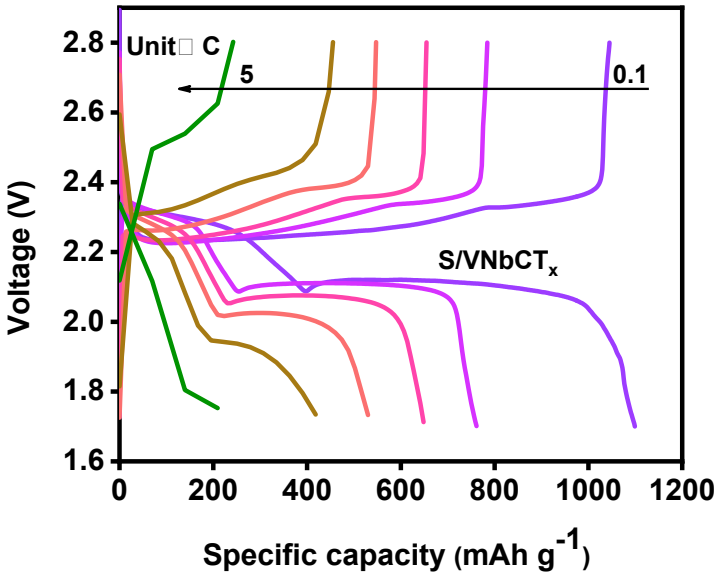

Fig. S14 GCD curves of the S/VNbCT$_x$ electrode at various current densities.

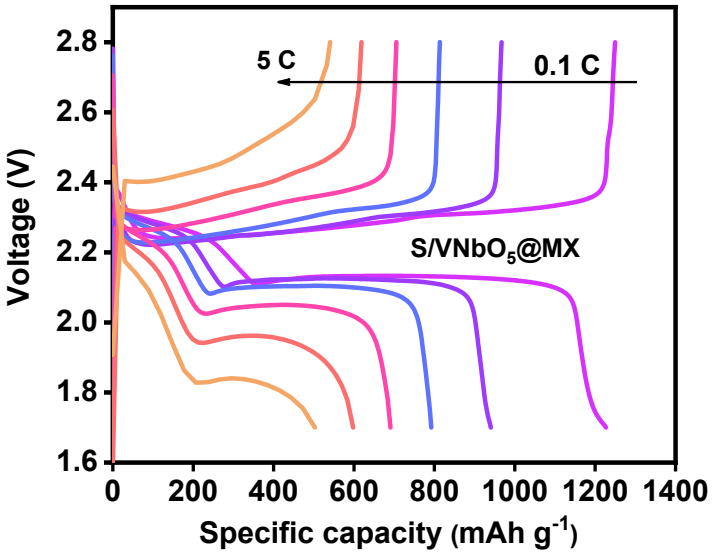

Fig. S15 GCD curves of the S/$VNbO_5$@MX electrode at various current densities.

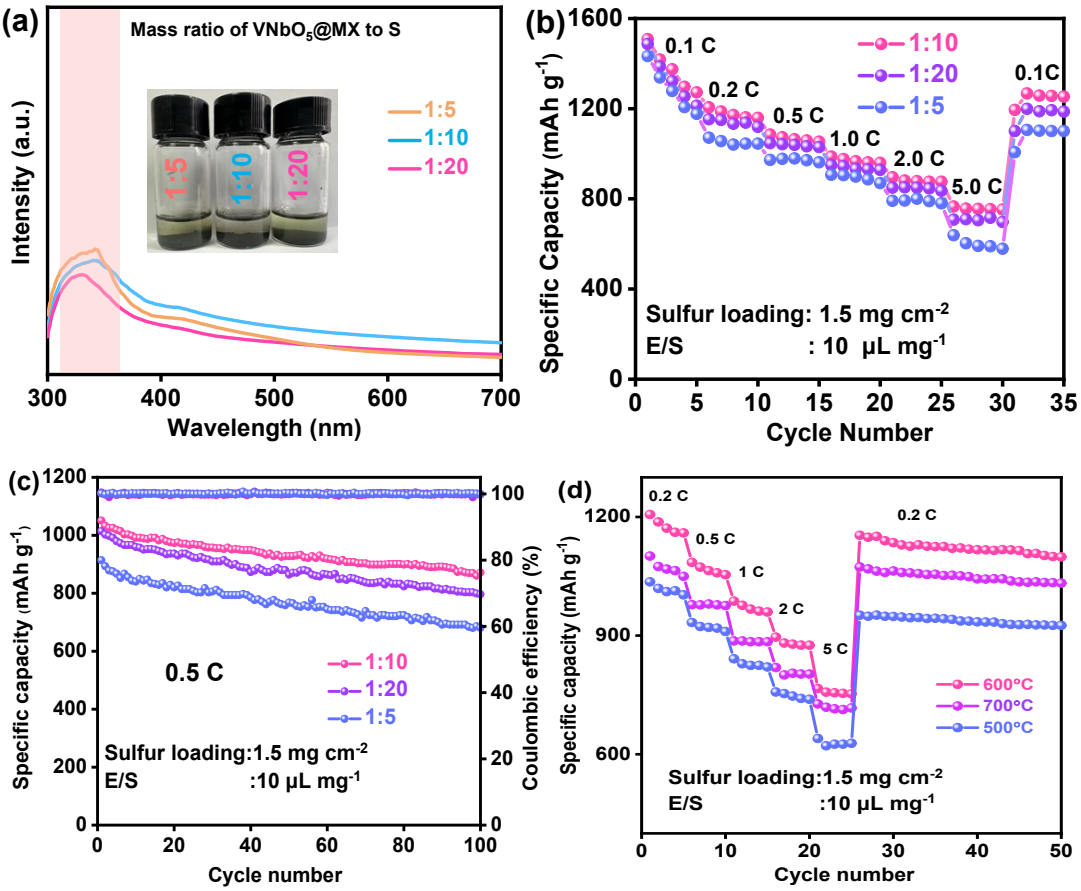

Fig. S16 (a) UV-vis spectra of the visual Li_2S_6 adsorption test for V_5S_8-Nb_2O_5@MX electrode prepared with different feeding ratios. (b) Cyclic performance of S/V_5S_8-Nb_2O_5@MX electrode with different feeding ratios. (c) Long-term cycling performance over 100 cycles at 0.5 C for S/V_5S_8-Nb_2O_5@MX electrode with different feeding ratios. (d) Cyclic performance of S/V_5S_8-Nb_2O_5@MX electrode prepared at 500, 600, and 700 °C.

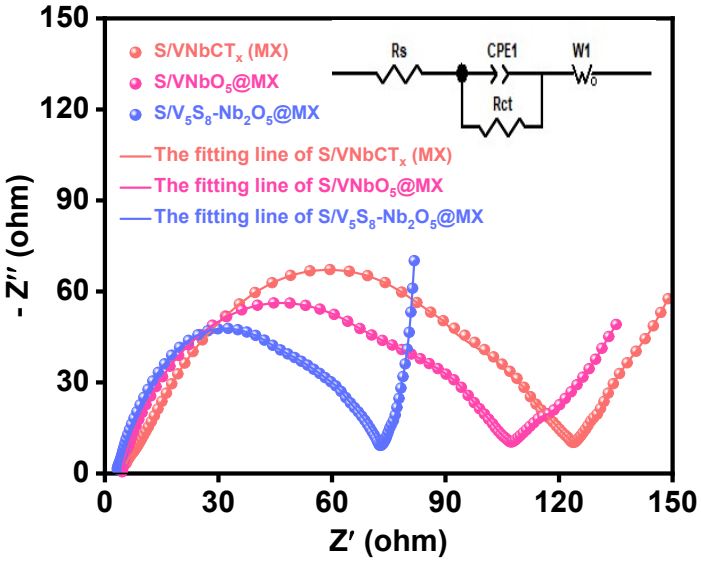

Fig. S17 Nyquist plots of different cells.

Table S1 Parameters of Langmuir, Freundlich and Liu adsorption isotherm models for polysulfide adsorption on V_5S_8-Nb_2O_5@MX, $VNbO_5$@MX and $VNbCT_x$ MXene adsorbents. R^2 is the adjusted coefficient of determination.

	Langmuir			Freundlich			Liu			
Materials	K_L (L/g)	Q_0 (mg/g)	R^2	K_F (mg/g)(L/mg)$^{1/n}$	n_s	R^2	K_{Liu} (L/g)	Q_0 (mg/g)	n_s	R^2
V_5S_8-Nb_2O_5@MX	14	236	0.92	20.44	0.45	0.78	18	221	4.42	0.98
$VNbO_5$@MX	9	175	0.96	10.53	0.39	0.95	15	168	1.93	0.99
$VNbCT_x$ MXene	23	141	0.89	22.54	0.16	0.91	10	140	0.64	0.94

Polysulfide adsorption isotherm models and calculations. Adsorption isotherms were fitted using the most common Langmuir, Freundlich, and Liu adsorption isotherm models given by equations (1), (2) and (3) [1].

Langmuir adsorption isotherm:
$$Q_e = \frac{Q_o K_L C_e}{1 + K_L C_e} \quad (1)$$

Freundlich adsorption isotherm:
$$Q_e = K_F C_e^{n_s} \quad (2)$$

Liu adsorption isotherm:
$$Q_e = \frac{Q_o (K_{Liu} C_e)^{n_s}}{1 + (K_{Liu} C_e)^{n_s}} \quad (3)$$

Where, $\boldsymbol{Q_e}$ is the amount of polysulfides adsorbed per gram of the materials adsorbe at equilibrium, $\boldsymbol{Q_o}$ is the maximum amount of polysulfides that can be adsorbed per gram of the materials adsorbent when the surface of materials (adsorbent) is fully covered with a monolayer Li_2S_6 molecules. $\boldsymbol{K_L}$, $\boldsymbol{K_F}$, and $\boldsymbol{K_{Liu}}$ are Langmuir, Freundlich and Liu equilibrium constant, representing the strength of interaction between polysulfides and materials. $\boldsymbol{C_e}$ is the equilibrium concentration (concentration of Li_2S_6 solution measured after subjected to adsorption test) and n_s represents the heterogeneity of the site energies.

Table S2 Kinetic parameters of the adsorption of LiPS by V_5S_8-Nb_2O_5@MX, $VNbO_5$@MX and $VNbCT_x$ MXene adsorbent. R^2 is adjusted coefficient of determination.

	Preudo first-order reaction			Preudo second-order reaction		
Absorbance	**K_1 (L/g)**	**Q_0 (mg/g)**	**R^2**	**K_2 (g·(mg·min)$^{-1}$)**	**Q_0 (mg/g)**	**R^2**
V_5S_8-Nb_2O_5@MX	1.11	230.73	0.97	0.08	255.32	0.99
$VNbO_5$@MX	0.74	185.82	0.90	0.05	214.46	0.95
$VNbCT_x$ MXene	2.10	130.28	0.98	0.44	136.06	0.99

Kinetic adsorption models and calculations. Adsorption kinetics of materials were fitted using the commonly used pseudo-first order, pseudo-second order and intraparticle diffusion models given by equations (4), (5) and (6), respectively [1].

Pseudo-first order: $$Q_t = Q_e\left(1 - e^{-k_1 t}\right) \quad (4)$$

Pseudo-second order: $$Q_t = \frac{Q_e^2 k_2 t}{Q_e K_2 t + 1} \quad (5)$$

Where, $\boldsymbol{Q_t}$ is the amount of polysulfides adsorbed at time $\boldsymbol{t}$, $\boldsymbol{Q_e}$ is the equilibrium adsorption capacity/maximum amount of polysulfides adsorbed on material under the conditions that adsorption tests were carried out, $\boldsymbol{k_1}$ and $\boldsymbol{k_2}$ are the pseudo-first order and pseudo-second order rate constants.

Table S3 Fitting results of the EIS plots.

	Rs (Ω)	Rct (Ω)	Chi-squarevalue	Estimated error(%)
S/VNbCT$_x$(MX)	3.29	126.21	2.07e-3	1.26
S/VNbO$_5$@MX	3.01	100.27	2.13e-2	2.95
S/V$_5$S$_8$-Nb$_2$O$_5$@MX	1.99	73.34	6.90e-3	0.29

Table S4 Comparison of V_5S_8-Nb_2O_5@MX heterostructure in this work with related reported work.

Materials	Sulfur Loading (mg cm^{-2})	Decay rate (cycles)	Maximum discharge capacity (mAh g^{-1})	References
V_5S_8-Nb_2O_5@MX	1.5	0.027% (500) at 1 C	1508(0.1 C)	This work
WS_2-WO_3@GN	1.2	0.04% (500) at 1 C	1137(0.3 C)	[2]
MXene@TiO_2	1.2	0.058% (500) at 2 C	1353(0.1 C)	[3]
Nb_2O_5-NbC/CNF	1.2	0.044% (800) at 1 C	1196(0.1 C)	[4]
MoS_2-MoN@CNT	-	0.041% (1000) at 2 C	1078(0.2 C)	[5]
VO_2-VN/Graphene	1.6-1.8	0.06% (800) at 2 C	1425(0.2 C)	[6]
1T-VS_2-MXene	1.2	0.079% (500) at 1 C	1378(0.1 C)	[7]
MoC@MoO_x-CFF	2.6	0.09% (200) at 0.2 C	~1200(0.2 C)	[8]

References

[1] G. Valurouthu, M. Shekhirev, M. Anayee, R.C. Wang, K. Matthews, T. Parker, R.W. Lord, D.Z. Zhang, A. Inman, M. Downes, C.W. Ahn, V. Kalr and Y. Gogotsi, Adv. Funct. Mater., 2024, 2404430.

[2] B. Zhang, C. Luo, Y.Q. Deng, Z.J. Huang, G.M. Zhou, W. Lv, Y.B. He, Y. Wan, F.Y. Kang and Q.H. Yang, Adv. Energy Mater., 2020, 10, 2000091.

[3] S.Y. Qiu, C. Wang, Z. X. Jiang, L.S. Zhang and L.L. Gu, Nanoscale, 2020, 12, 16678-16684.

[4] Z.X. Cao, J. Guo, S.N. Chen, Z.N. Zhang, Z.P. Shi, Y.H. Yin, M.G. Yang, X.X. Wang and S. Yang, J. Mater. Chem. A, 2021, 9, 21867-21876.

[5] S. Wang, S. Feng, J. Liang, Q. Su, F. Zhao, H. Song, M. Zheng, Q. Sun, Z. Song, X. Jia, J. Yang, Y. Li, J. Liao, R. Li and X. Sun, Adv. Energy Mater., 2021,11, 2003314.

[6] Y. Song, W. Zhao, L. Zhang, X. Zhu, Y. Shao, F. Ding, J. Sun and Z. Liu, Energy Environ. Sci., 2018, 11, 2620-2630.

[7] S. Wu, W. Wang, J. Shan, X. Wang, D. Lu, J. Zhu, L. Yue and Y. Li, Energy Storage Mater., 2020, 49, 153-163.

[8] R. Fang, S. Zhao, Z. Sun, D.W. Wang, R. Amal, S. Wang, H.M. Cheng and F. Li, Energy Storage Mater., 2018, 10, 56-61.